

## **Arabinogalactan as a Green Inhibitor for Carbon Steel Corrosion in 1M HCL Solution**

**Marziya Rizvi**

Department of Applied Chemistry, Aligarh Muslim University, Aligarh-202002, India  
marziyarizvi@gmail.com

**Mohammad Mobin**

Department of Applied Chemistry, Aligarh Muslim University, Aligarh-202002, India

### **ABSTRACT**

Biopolymer arabinogalactan (AG) was investigated for its inhibition characteristics for carbon steel (CS) corrosion in 1M HCl. Gravimetric method, electrochemical impedance spectroscopy (EIS), potentiodynamic polarization measurements (PDP) and Atomic Force Microscopy (AFM) assessed the inhibition and adsorption of AG in the acid solution. The studies proved that the inhibition efficiency increased with elevating temperature and increasing AG concentration in acid solution. AG adsorption on CS favored Langmuir adsorption isotherm. Results of corrosion tests confirmed that AG could serve as efficient green inhibitor for CS corrosion in 1 M HCl with high inhibition efficiency and a low risk of environmental pollution. Monte Carlo simulation and theoretical quantum chemical studies were used to corroborate experimental results.

*Keywords: Green Inhibitor, Gravimetric Analysis, Electrochemical analysis, DFT, AFM*

**NIGIS \* CORCON 2017 \* 17-20 September \* Mumbai, India**

Copyright 2017 by NIGIS. The material presented and the views expressed in this paper are solely those of the author(s) and do not necessarily by NIGIS.

## INTRODUCTION

In acidic environments the usage of inorganic/organic inhibitors of carbon steel corrosion is well established. Unfortunately, most of them are expensive, toxic towards the environment and non-biodegradable. The adversely affecting chemicals and recent increase in environmental awareness has geared the research activities towards development of cheap, non-toxic, environment friendly and biodegradable substances as corrosion inhibitors. These pre-requisites are fulfilled by the natural polymers which function as effective corrosion inhibitors of metals in diverse degradative environments. Few of the natural polymers, which have been studied as green inhibitors for carbon steel corrosion in acid solutions in the recent past include: carboxymethyl cellulose, starch, Gum Arabic, chitosan pectin and xanthan gum. However, low to moderate inhibition efficiency is amongst the limiting factors attributed to the employment of natural polymers as corrosion inhibitors. Several attempts such as synergizing with halide additives copolymerization, cross linking and composite formation.

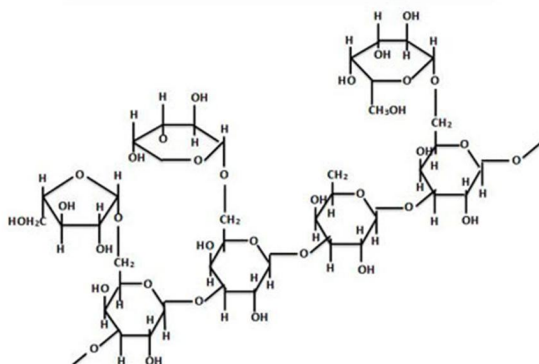


**Figure S1. Molecular structure of arabinogalactan**

AG is complex, hydrophilic, heterogeneous and a highly branched anionic polysaccharide comprised of L-arabinose, D-galactose, D-xylose, L-rhamnose, D-glucose, L-fucose and D-galacturonic acid<sup>1-3</sup>. There are many research articles on the polysaccharides as corrosion inhibitors of metal in aggressive solutions like ones discussed above, but no published facts are known on AG as inhibitor for A1020 c-steel corrosion in 1M HCl. In the current work, AG has been selected as eco-friendly corrosion inhibitor for carbon steel in 1M HCl. The main constituents of AG, has numerous of hydroxyl group ( $-OH$ ) and heteroatom O. The aim of this evaluation is to assess the improvement of corrosion resistance of A1020 carbon steel by AG in 1M HCl using gravimetric, electrochemical and surface analysis in order to clarify its inhibition mechanism. Electron density distributions in AG molecule and its reactivity indices obtained from density functional theory calculations were reported. Adsorption of AG molecule on carbon steel (represented by Fe(110)) was modeled with the Monte Carlo simulation approach<sup>1-3</sup>.

## EXPERIMENTAL PROCEDURE

### SPECIMEN PREPARATION

The corrosion tests were executed on coupons obtained from A1020 c-steel chemically composed of 0.0684 % C, 0.0394% Mn, 0.0008% S, 0.0219% P, 0.0456% Cr, 0.0674% Mo, 0.0154% Al, 0.0335% V and remainder Fe (in weight%). A1020 carbon steel's chemical constitution was measured by spark optical emission spectrometer. Rectangular coupons [2.5 × 2 × 0.1 cm and surface area: 10.9 cm<sup>2</sup>] were employed for gravimetric measurements. Circular coupons with 1.0 cm<sup>2</sup> exposed surface area (thickness 0.1 cm) were used for electrochemical analysis. The coupons were abraded by emery papers of various grades, washed with acetone and later with de-ionized water and lastly dried at room temperature before performing corrosion tests on them.

### ELECTROLYTIC SOLUTION

AR grade 37% HCl was diluted with double-distilled water to prepare electrolytic solution of 1 M HCl. The concentration of AG in the 1M HCl solution was varied between 100ppm-500 ppm. The electrolytic volume used in gravimetric and electrochemical measurements was 200 mL and 1 L, respectively.

### GRAVIMETRIC MEASUREMENTS

The freshly abraded coupons of carbon steel were completely immersed in 1 M HCl for 6 h. The test solutions contained different concentrations of the AG at temperatures 30°C, 40°C, 50°C and 60°C, respectively. The carbon steel coupons were thoroughly rinsed by de-ionized water, gently scrubbed by a bristle brush to remove the corrosion products, washed successively with de-ionized water and acetone and finally dried to a constant weight. The gravimetric measurements were conducted on triplicate specimens to ascertain the reproducibility of results and average corrosion rate was computed. Corrosion rate calculation in 'mg cm<sup>-2</sup> h<sup>-1</sup>' was done using the following equation:

$$\text{Corrosion rate (mg cm}^{-2} \text{ h}^{-1}) = \frac{\Delta W}{A t} \quad (1)$$

where  $\Delta W$ , is weight loss (mg),  $A$ , is the area of specimen (cm<sup>2</sup>) and  $t$ , is exposure time (h). The % inhibition efficiency represented by ' $\eta$ ' was obtained using average corrosion rate as follows:

$$\eta = \frac{CR_0 - CR_i}{CR_0} \times 100 \quad (2)$$

where  $CR_0$  and  $CR_i$  were the corrosion rates in free and acid solutions inhibited by AG.

### ELECTROCHEMICAL MEASUREMENTS

The electrochemical measurements were executed on Autolab 128N Potentiostat/Galvanostat. A three neck corrosion cell from AUTOLAB (capacity 1L) that includes test coupon of vulnerable surface area of 1cm<sup>2</sup>, embedded in specimen holder as working electrode (WE), Ag/AgCl electrode (saturated KCl) as reference electrode (RE) and platinum foil as counter electrode (CE) was used

**NIGIS \* CORCON 2017 \* 17-20 September \* Mumbai, India**

Copyright 2017 by NIGIS. The material presented and the views expressed in this paper are solely those of the author(s) and do not necessarily by NIGIS.

during the experiments. Before starting the electrochemical measurements, the *WE* was stationed in the test solution and the rest potential was ceaselessly observed until it was stabilized and a steady state potential was achieved. Approximately one hour of immersion was sufficient to stabilize the potential and establish a steady state open circuit potential (OCP). All the experiments were performed under aerated, unstirred conditions at room temperature (30°C ± 1°C). The potentiodynamic polarization method recorded the polarization curves from -250 to +250 mV with respect to steady state OCP at a scan rate of 0.00166 V/s. The corrosion current density ( $i_{\text{corr}}$ ), anodic Tafel slope ( $\beta_a$ ), cathodic Tafel slope ( $\beta_c$ ) and corrosion potential ( $E_{\text{corr}}$ ) were obtained. Cathodic and anodic polarization curves were analysed using NOVA 1.11 software. The measured  $i_{\text{corr}}$  values helped in the calculation of inhibition efficiency  $\eta$  (%) as per the following relationship:

$$\eta(\%) = \frac{i_{\text{corr}}^0 - i_{\text{corr}}}{i_{\text{corr}}^0} \times 100 \quad (3)$$

where,  $i_{\text{corr}}$  and  $i_{\text{corr}}^0$  represent the corrosion current densities in the presence and absence of AG. Frequency spectrum from  $10^{-2}$  to  $10^4$  Hz and ac signals of 10 mV amplitude was employed to conduct the impedance measurements. Nova 1.11 software assisted in obtaining and analyzing the impedance parameters. The % inhibition efficiency ' $\eta$ ' was obtained using charge transfer resistance ( $R_{\text{ct}}$ ) in the impedance data of the Nyquist plots

$$\eta(\%) = \left( \frac{R_{\text{ct}} - R_{\text{ct}}^0}{R_{\text{ct}}} \right) \times 100 \quad (4)$$

Here,  $R_{\text{ct}}$  and  $R_{\text{ct}}^0$  were the charge transfer resistance values inclusive and exclusive of AG, respectively.

## SURFACE ANALYSIS

To visually assess the corrosion extent on the carbon steel specimens (in terms of heterogeneity of the surface/roughness) immersed in uninhibited/inhibited acid solution, the surface analysis was performed by AFM. These analyses were performed on test coupons obtained from weight loss experiments inclusive and exclusive of optimum concentration of AG at 30°C. The instrument incorporated to conduct AFM of uninhibited and inhibited carbon steel specimens was 'Dimension icon ScanAsyst' having spring constant of 42 Nm<sup>-1</sup> and tip radius 10 nm. A scan rate of 0.4 Hz was used for studying an area of 50 x 50 µm<sup>2</sup> of test coupon in tapping mode. The data obtained was analysed by Nanoscope V software.

## QUANTUM CHEMICAL STUDIES

Density functional theory (DFT) method was used to derive the electron density distributions and obtain important quantum chemical parameters of AG molecule. The generally accepted molecular unit of AG (as found in PubChem) was used as the representative molecular structure for all computational studies. B3LYP/6-31G(d,p) model achieved the gas phase optimized geometry of the molecule. Gaussian 09 software suite performed the calculations. The highest occupied molecular orbital energy ( $E_{HOMO}$ ) and the lowest unoccupied molecular orbital ( $E_{LUMO}$ ) energy, and dipole moment were recorded. The energy gap ( $\Delta E$ ), global hardness ( $\eta$ ), and global electronegativity ( $\chi$ ) of the molecule were calculated using the appropriate relations :

$$\Delta E = E_{LUMO} - E_{HOMO} \quad (5)$$

$$\eta = \frac{1}{2}(E_{LUMO} - E_{HOMO}) \quad (6)$$

$$\chi = \frac{1}{2}(E_{HOMO} + E_{LUMO}) \quad (7)$$

Electrophilic ( $f^+$ ) and nucleophilic ( $f^-$ ) Fukui indices of the molecules were estimated using the Mulliken atomic charge differences based on the relations:

$$f^+ = q_{N+1} - q_N \quad (8)$$

$$f^- = q_N - q_{N-1} \quad (9)$$

Electron density distributions of the Fukui functions were visualized using the Multiwfn software

## RESULTS

### GRAVIMETRIC MEASUREMENTS

Enlisted in Table 1 are the corrosion values obtained by gravimetric measurements that prove AG to be an efficacious inhibitor of carbon steel degradation in 1M HCl solution at temperatures between 30°C and 60°C. With increasing AG concentration and the test solution temperature, the inhibition efficiency increases; the maximum inhibition efficiency of 96.30% is observed at 60° C at AG concentration of 500ppm.

**Table 1.** Corrosion parameters for carbon steel in 1 M HCl in absence and presence of different concentrations of AG at 30-60°C from gravimetric analysis.

AG Conc. (ppm)	Corrosion Rate (mg cm <sup>-2</sup> h <sup>-1</sup> )				$\eta$ (%)			
	30°C	40°C	50°C	60°C	30°C	40°C	50°C	60°C
Blank	0.86	1.39	3.73	4.86	-	-	-	-
100	0.26	0.38	0.91	1.11	70.24	72.43	75.71	77.15
200	0.18	0.26	0.62	0.69	79.51	81.32	83.28	85.78
300	0.16	0.22	0.51	0.58	81.45	84.33	86.31	88.14
400	0.10	0.15	0.33	0.33	88.00	89.16	91.04	93.15
500	0.06	0.08	0.16	0.18	93.31	94.57	95.77	96.30

AG molecules adsorb on the surface of carbon steel, construct a barrier for the mass and charge transfers as the inhibitor concentration increase. This further leads to the inhibition of the attack of the aggressive 1M HCl on the carbon steel surface.

The degree of protection against acid attack is directly related to the surface fraction covered by the adsorbed AG. As the AG concentration is increased, the number of the adsorbed molecules increases on the surface, resulting in better protection. A parameter surface coverage,  $\theta$ , could be used to define the fraction of the carbon steel surface occupied by the adsorbed molecules. The surface coverage can be calculated using the formula:

$$\theta = \frac{CR_0 - CR_i}{CR_0} \quad (10)$$

where  $CR_0$  is corrosion rate in uninhibited acid solution and  $CR_i$  is corrosion rate in inhibited acid solution. Inspecting Table 1, an inference is derived that the surface coverage increases with increasing AG concentration. AG inhibits carbon steel corrosion at all temperatures evaluated. The increasing inhibition efficiency with increase in the test solution's temperature suggests a chemical nature of adsorption of AG molecules in 1M HCl solution. As the test solution temperature increases the de-sorption of the water from metal surface is more favored resulting in the availability of larger surface area and increased adsorption of AG molecules<sup>4</sup>.

## ELECTROCHEMICAL MEASUREMENTS

### Potentiodynamic Polarization Measurements

Investigating the mechanism and the kinetics of cathodic and anodic reactions, potentiodynamic measurements were performed. Figure 2 (a) shows the polarization curves for carbon steel in 1M HCl adding and excluding different concentrations of AG. The polarization parameters deduced have been recorded in Table 2

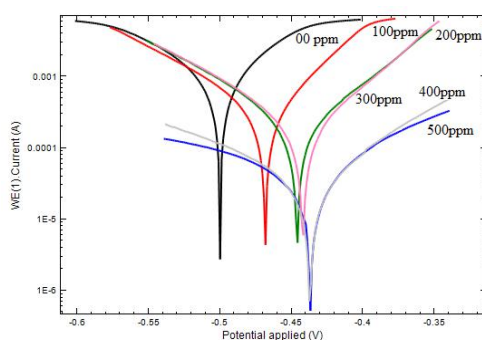
**NIGIS \* CORCON 2017 \* 17-20 September \* Mumbai, India**

Copyright 2017 by NIGIS. The material presented and the views expressed in this paper are solely those of the author(s) and do not necessarily by NIGIS.

**Table 2.** Potentiodynamic polarization parameters for corrosion of carbon steel in 1M HCl in absence and presence of AG at 30°C.

AG Conc. (ppm)	$E_{\text{corr}}$ (mV, Ag/AgCl)	$i_{\text{corr}}$ ( $\mu\text{Acm}^{-2}$ )	$\beta_a$ (mVdec $^{-1}$ )	$\beta_c$ (mVdec $^{-1}$ )	$R_p$ ( $\Omega \text{ cm}^{-2}$ )	CR (mmpy)	$\eta$ (%)
0	-500.07	1208.5	103.46	82.79	16.53	14.04	-
100	-468.49	363.25	91.08	61.98	44.09	4.22	69.9
200	-446.21	256.84	92.71	86.86	75.83	2.98	78.7
300	-442.19	241.17	95.36	79.49	78.07	2.80	80.1
400	-442.79	141.27	121.02	72.14	138.96	1.64	88.3
500	-437.22	39.62	116.97	88.37	551.7	0.46	96.7

On adding AG to 1M HCl,  $E_{\text{corr}}$  values become more positive and shift anodically compared to the blank. Observing the magnitude of change observed in the  $E_{\text{corr}}$  values we can say that AG is a mixed type inhibitor predominantly anodic in nature, i.e., presence of AG inhibited oxidation of Fe and to a lower extent hydrogen evolution. A progressive decrease in the value of  $i_{\text{corr}}$  was observed as the AG concentration was increased, suggesting a retarded rate of electrochemical reaction, as a barrier was created between metal and corrosive HCl solution by protective AG film on the carbon steel surface. The variation in the values of  $\beta_c$  and  $\beta_a$  in the 1 M HCl having AG indicates that both the cathodic hydrogen evolution and anodic metal dissolution processes are inhibited. An increase in the polarization resistance ( $R_p$ ) occurs on AG addition. The increasing values of  $R_p$  with increasing inhibitor concentration, suggest effective corrosion inhibition by AG. The highest value of inhibition efficiency of 96.7% was observed at AG concentration of 500ppm. The inhibition efficiencies calculated by polarization measurements exhibit the trend parallel to that of gravimetric measurements<sup>4</sup>.



(a)

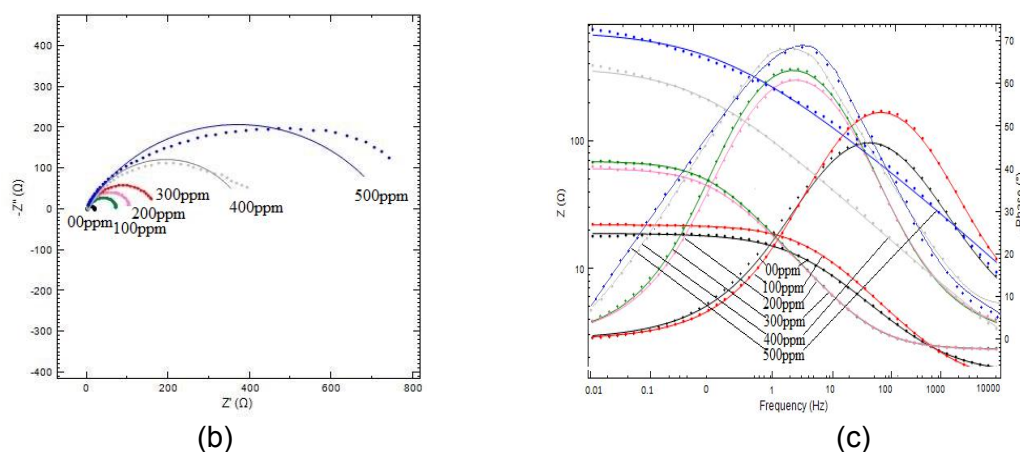


**Figure 2. (a) Potentiodynamic polarization curves (b) Nyquist and (c) Bode plots for carbon steel sample in 1M HCl in absence and presence of various concentrations of AG**

### ***Electrochemical Impedance Spectroscopy (EIS)***

The electrochemical impedance spectroscopy evaluated the corrosion inhibition in presence and absence of AG's various concentrations. The impedance data for low carbon steel in 1M HCl solution exclusive and inclusive of AG obtained at 30°C is enlisted in Table 3. The semicircle fitting method determined the electrochemical impedance parameters. The Nyquist plots for carbon steel's surface inhibited by AG comprised of a depressed semicircle with a high-frequency capacitive loop (Figure 2 b). Due to the state of the electrode surface and the dispersion effect, which is a characteristic impedance property of carbon steel electrodes in the process of corrosion, a diversion from a the perfect semicircle – a depressed semicircle in the center under the real axis was observed, which was primarily caused by heterogeneity and roughness of the electrode surface and also by the geometrical behavior of the current distribution. The impedance response changed considerably after the addition of AG to the 1M HCl solution. Shapes of the plots remained same for the electrodes with and without various AG concentrations indicating an unaltered mechanism of corrosion on addition of AG <sup>5</sup>.



**Table 3. EIS parameters for corrosion of carbon steel in 1 M HCl in absence and presence of AG at 30°C**

AG Conc. (ppm)	Rs (Ω/cm <sup>2</sup> )	R <sub>ct</sub> (Ω/cm <sup>2</sup> )	CPE		C <sub>dl</sub> × 10 <sup>-5</sup> (μFcm <sup>-2</sup> )	η(%)	χ <sup>2</sup> × 10 <sup>-3</sup>	-S	α'
			Y <sub>0</sub> × 10 <sup>-6</sup> (Ω <sup>-1</sup> s <sup>n</sup> cm <sup>2</sup> )	n					
0	1.6	17.48	79.4	0.991	7.5	-	2.40	1.42	46.2
100	2.3	70.03	71.8	0.995	7.4	75.1	1.82	1.46	56.8
200	2.4	103.36	66.1	0.995	6.5	83.1	3.43	1.52	59.5
300	3.1	169.71	51.4	0.996	5.1	89.7	3.88	1.53	61.2
400	3.6	416.3	36.7	0.996	3.6	95.8	12.15	1.64	61.5
500	2.2	961.2	19.1	0.996	1.9	98.1	41.57	1.81	75.1

Nova 1.11 Software (Metrohm Corporation) measured and simulated the electrochemical impedance spectra on the carbon steel/1M HCl interface with and without AG by fitting various impedance profiles into an equivalent circuit which is given in Figure S5 (Supporting Information). This equivalent circuit is comprised of constant phase element, CPE, solution resistance,  $R_s$  and charge transfer resistance,  $R_{ct}$ . The system investigated here can be characterized by distributed capacitance for a non homogenous corroding surface of carbon steel in 1 M HCl. This phenomenon of depression modeled by CPE is usually associated with the frequency dispersion, dislocations, and surface roughness, formation of porous layers and distribution of the active sites. The distributed capacitance is given by constant phase element (CPE,  $Y_0$ )<sup>6</sup>. The CPE's impedance is given as:

$$Z_{CPE} = \frac{1}{Y_0 (j\omega)^n} \quad (15)$$

Here, the angular frequency ' $\omega$ '; an imaginary number ' $j^2 = -1$ '; magnitude of CPE ' $Y_0$ ' is the; and the CPE exponent ' $n$ '. When  $n = -1$ , CPE is an inductor and a pure capacitor when  $n = 1$ . The values of  $C_{dl}$  were calculated at a frequency at which the imaginary component of the impedance is a maximum:

$$C_{dl} = Y_0 (\omega_{max})^{n-1} \quad (16)$$

Table 3 clearly indicates that the values of  $R_{ct}$  increased and that of  $C_{dl}$  decreased with increased AG concentration. Increase in the thickness of the double layer and/or decrease in dielectric constant cause a decrease in the  $C_{dl}$  value. An inhibitive layer on the electrode surface controlled the dissolution extent by displacing the H<sub>2</sub>O and other ions that were initially adsorbed on steel/solution interface. Fe-H<sub>2</sub>O complex that developed on steel surface in presence of uninhibited 1M HCl changes to Fe-AG complex which formed in on addition of AG to the acid solution. Due to AG adsorption on the active sites of the carbon steel surface, surface heterogeneity reduces and value of ' $n$ ' gets closer to unity. At a concentration of 500 ppm AG becomes 98.1 % efficient. Ideally the  $\chi^2$  values lie between 10<sup>-3</sup> and 10<sup>-5</sup><sup>7</sup>. In the current study the  $\chi^2$  values for AG adsorption are within 10<sup>-3</sup>. The impedance measurements resulted in inhibition efficiencies quite similar that of the gravimetric and potentiodynamic polarization studies. The inhibitory effect of the compound may be

**NIGIS \* CORCON 2017 \* 17-20 September \* Mumbai, India**

Copyright 2017 by NIGIS. The material presented and the views expressed in this paper are solely those of the author(s) and do not necessarily by NIGIS.

judged by phase angle at high frequencies in phase angle vs. frequency diagrams which are given in the Bode plots in Figure 2c. Addition of AG renders a higher protection with higher values of absolute impedance at low frequencies. In theta vs. frequency diagram (Figure 2c), a more negative phase angle means higher capacitive behavior intermediate frequency region. The analyses of linear relationship between  $\log |Z|$  versus  $\log f$  give a slope value between -1.42 and -1.81<sup>8</sup>.

## ATOMIC FORCE MICROSCOPY (AFM)

AFM quantitatively analyzed the morphologies of the corrosion inhibition of carbon steel coupons immersed in 1M HCl for 6 h in the presence and absence of AG (Figure 3). The AFM image of freshly abraded carbon steel specimen in Figure 3(a), displays a sufficiently smooth surface. Another AFM image of severely corroded surface of carbon steel immersed in test solution for 6 h at 30°C is shown in Figure 3(b). The image in Figure 3(c) shows a surface even and smooth in the presence of 500ppm AG comparative to the image obtained for coupon immersed in uninhibited solution. The polished steel surface before immersion in test solution exhibited an average roughness of 71.4nm. A quite high roughness of 781 nm was observed on the carbon steel surface immersed in 1M HCl without AG [Figure 3(b)]. For the steel specimen immersed in test solution of 1 M HCl having 500 ppm AG there is very less corrosion damage present on the surface depicted by small spikes as seen in Figure 3(c) and average roughness of 77.7 nm is obtained which indicated the adsorption of microscopically thin film of AG preventing the attack of corrosive acid solution.

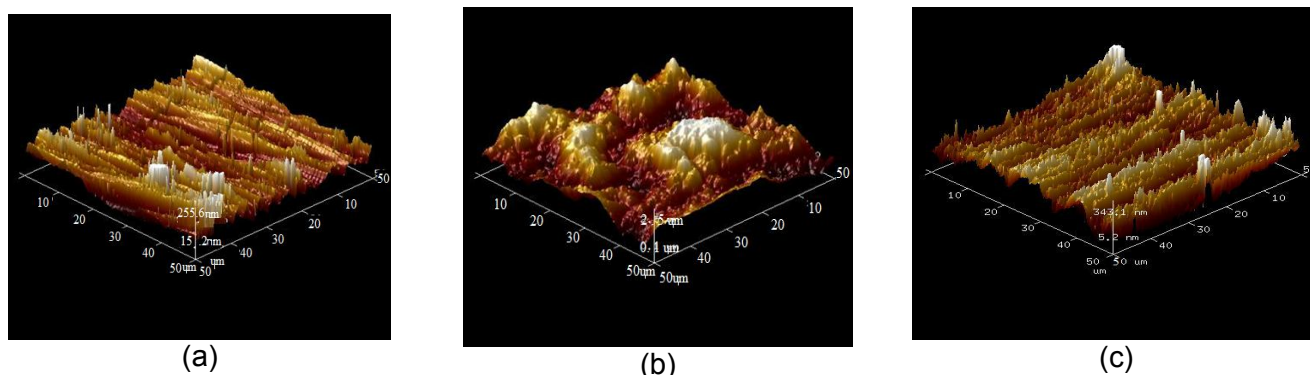


**Figure 3. 3D AFM and SEM/EDX images of carbon steel prior to and after immersion in test solution for 6 h at 30° C; (a), (d) and (g) as ground before immersion; (b), (e) and (h) uninhibited solution and (c), (f) and (i) inhibited solution (500ppm AG)**

## Quantum Chemical Calculations and Monte Carlo Simulations

Gas phase optimized geometry of AG molecule and graphical images of electron density distributions in its HOMO, LUMO, electrophilic and nucleophilic Fukui indices are shown in Figure 4. The HOMO lobes are located on the pyran ring with larger fractions on the O-atoms of the –OH and –OCH<sub>3</sub> groups. The LUMO comprises a large lobe that is centered on an hydroxylmethylene group on one of the pyran rings. These observations suggest that the molecule is liable to interact with metallic orbitals using mainly the centers with O-atoms. The HOMO and LUMO surfaces and contours for AG suggest a non-uniform distribution of electron density around the molecule,

**NIGIS \* CORCON 2017 \* 17-20 September \* Mumbai, India**

Copyright 2017 by NIGIS. The material presented and the views expressed in this paper are solely those of the author(s) and do not necessarily by NIGIS.

indicating the AG molecule is non-symmetric, and the molecule may not exhibit uniform reactivity on all the pyran rings.

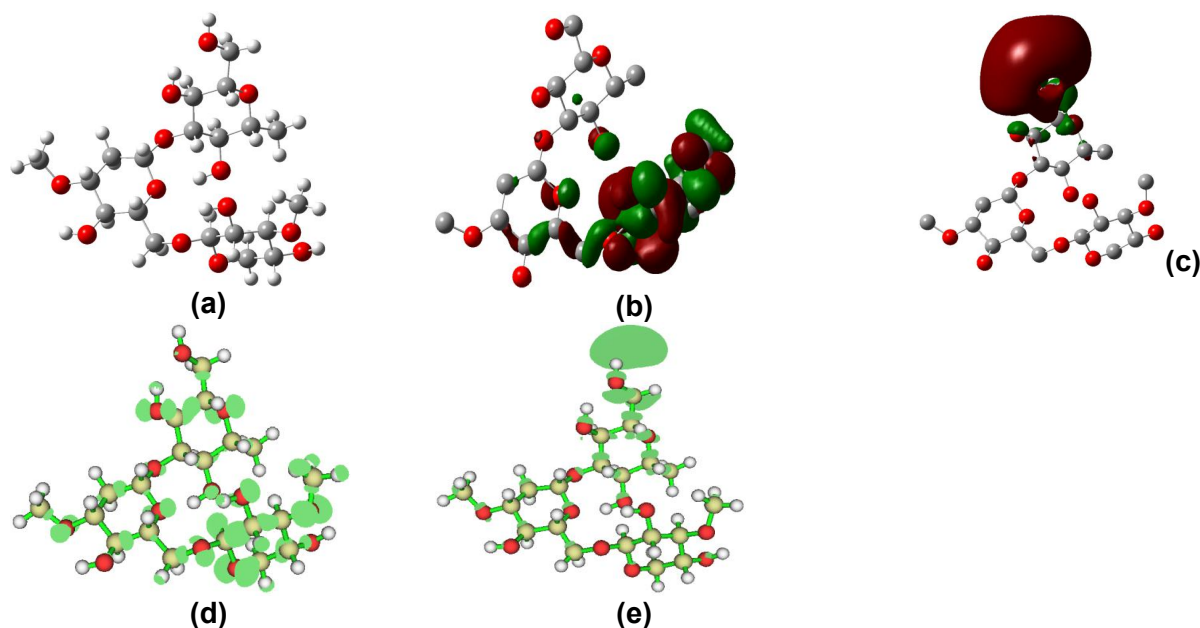


**Figure 4.** Optimized structure (a); HOMO (b) and LUMO (c) electron density; and (d)  $f^-$  and  $f^+$  (e) Fukui indices electron density isosurfaces for AG

The  $f^-$  further confirms that the centers for electrophilic attacks on AG molecule are essentially the O-atoms with  $\sigma$ -characteristic orbitals. The  $f^+$  also corroborates the observation from the LUMO contour surface, showing the hydroxylmethylene group with superior disposition towards nucleophilic attack. Selected quantum chemical parameters of the molecule are shown in Table 4.

**Table 4.** Quantum chemical parameters obtained using B3LYP/6-31G(d,p) model and energy parameters (kJ/mol) for the adsorption of AG on Fe (110) surface

Quantum chemical parameters	
$E_{\text{HOMO}}$	-6.943
$E_{\text{LUMO}}$	-0.547
$\Delta E$	6.396
$\eta$	3.198
$\chi$	3.745
Dipole moment	6.955

**NIGIS \* CORCON 2017 \* 17-20 September \* Mumbai, India**

Copyright 2017 by NIGIS. The material presented and the views expressed in this paper are solely those of the author(s) and do not necessarily by NIGIS.

The  $E_{\text{LUMO}}$  is somewhat high, which suppresses the possibility of back-bonding in interactions of AG molecule with steel. The large dipole moment (6.955 Debye) of AG molecule might favour dipole-dipole interactions with polarized steel surface<sup>9</sup>.

## INHIBITION MECHANISM

The adsorption of the biopolymer occurs by its electrostatic interaction with positively charged carbon steel surface or via lone pair interaction between heteroatom O and vacant orbital of Fe on surface of CS.

## CONCLUSIONS

- i. AG efficiently inhibits the corrosion of carbon steel coupon in 1 M HCl solution. The inhibition efficiency is both concentration and temperature reliant and reaches as high as 96.3 %.
- ii. High values of  $C_{\text{dl}}$  (the double layer capacitance) in the inhibited acid solution, with an accompanying increase in  $R_{\text{ct}}$  (charge transfer resistance) with respect to blank solution indicates the accumulation of protective AG layer at the metal/solution interface.
- iii. The Tafel plots suggest that AG act as mixed-type inhibitor for carbon steel in 1M HCl solution with a predominantly anodic effect.
- iv. AFM micrographs revealed that in-homogeneity of carbon steel surface was considerably homogenised by AG giving a clear evidence of its adsorption on carbon steel surface and the high protection it offers in 1 M HCl solution.
- v. Theoretical quantum chemical studies provided corroborative explanation to the observed inhibitive performance of AG.

## ACKNOWLEDGMENTS

One of the authors Marziya Rizvi thanks UGC, New Delhi for the financial assistance in the form of Maulana Azad National Fellowship. The author also thanks USIF, AMU, Aligarh, India, for analysis by SEM/EDX, NRF, IIT-D, New Delhi, India for assistance in surface analysis by AFM and CDRI Lucknow India for NMR.

**NIGIS \* CORCON 2017 \* 17-20 September \* Mumbai, India**

Copyright 2017 by NIGIS. The material presented and the views expressed in this paper are solely those of the author(s) and do not necessarily by NIGIS.

## REFERENCES

- 1) Tischer, C. A.; Iacomini, M.; Gorin Philip A.J. Structure of the arabinogalactan from gum tragacanth (*Astragalus gummifer*). *Carbohydrate Research*, 337, 1647–1655, 2002.
- 2) Fattahi, A; Petrini, P; Munarin, F; Shokoohinia, Y; Golozar, M. A.; Varshosaz, J; Tanzi M. C. Polysaccharides Derived from Tragacanth as Biocompatible Polymers and Gels *J. Appl. Polym. Sci.*, 129, 2092-2102, 2013.
- 3) Bouklah, M.; Hammouti, B.; Lagrene'e, M.; Bentiss, F. Thermodynamic properties of 2,5-bis(4-methoxyphenyl)-1,3,4-oxadiazole as a corrosion inhibitor for mild steel in normal sulfuric acid medium. *Corrosion Science*. 48, 2831–2842, 2006.
- 4) Ahamad, I.; Prasad, R.; Quraishi, M. A. Experimental and Theoretical Investigations of Adsorption of Fexofenadine at Mild Steel/Hydrochloric Acid Interface as Corrosion Inhibitor. *J. Solid State Electrochem.* 14, 2095-2099, 2010.
- 5) Mourya, P.; Banerjee, S.; Singh, M.M. Corrosion inhibition of carbon steel in acidic solution by *Tagetes erecta* (Marigoldflower) extract as a green inhibitor. *Corrosion Science*, 85, 352-363, 2014.
- 6) El-Lateef, Abd. Experimental and computational investigation on the corrosion inhibition characteristics of mild steel by some novel synthesized imines in hydrochloric acid solutions. *Corrosion Science*, 92, 104-117, 2015.
- 7) Scully, J. R.; Silverman, D. C.; Martin, K. W. Electrochemical Impedance: Analysis and Interpretation, Issue 1188, ASTM Publication (PCN04-011880-27): Fredericksburg, V.A., pp 433-435, 1993.
- 8) Zhang, Bingru; He, Chengjun; Chen, Xi; Tian, Zhipeng; Li, F. The synergistic effect of polyamidoamine dendrimers and sodium silicate on the corrosion of carbon steel in soft water. *Corrosion Science*, 90, 585–596, 2015.
- 9) Frisch, M. J.; Trucks, G. W.; Schlegel, H. B.; Scuseria, G. E.; Robb, M. A.; Cheeseman, J. R.; Scalmani, G.; Barone, V.; Mennucci, B.; Petersson, G. A.; *et al.* 2009, Gaussian 09, Revision D.01; Gaussian, Inc.: Wallingford CT.